Reduced exchange narrowing caused by gate-induced charge carriers in high-mobility donor–acceptor copolymers

Jun'ya Tsutsumi, Satoshi Matsuoka, Itaru Osaka, Reiji Kumai, and Tatsuo Hasegawa

Phys. Rev. B **95**, 115306 — Published 13 March 2017

DOI: 10.1103/PhysRevB.95.115306

Reduced Exchange Narrowing Caused by Gate-Induced Charge Carriers in High-Mobility Donor–Acceptor Copolymers

Jun'ya Tsutsumi,[1] Satoshi Matsuoka,[1,2] Itaru Osaka,[3,4] Reiji Kumai,[5] and Tatsuo Hasegawa[1,6]

[1]*National Institute of Advanced Industrial Science and Technology (AIST), 1-1-1 Higashi, Tsukuba 305-8565, Japan*

[2]*Department of Chemistry, Faculty of Pure and Applied Sciences, University of Tsukuba, Tsukuba 305-8571, Japan*

[3]*Department of Applied Chemistry, Graduate School of Engineering, Hiroshima University, Higashi-Hiroshima 739-8527, Japan*

[4]*Emergent Molecular Function Research Group, RIKEN Center for Emergent Matter Science (CEMS), Wako, Saitama 351-0198, Japan*

[5]*Condensed Matter Research Center (CMRC) and Photon Factory, High Energy Accelerator Research Organization (KEK), Institute of Materials Structure Science, Tsukuba 305-0801, Japan*

[6]*Department of Applied Physics, The University of Tokyo, Tokyo 113-8656, Japan*

ABSTRACT

Variations in exciton absorption resulting from charge accumulation in various semiconducting donor–acceptor (DA) copolymer thin films were systematically investigated by gate-modulation (GM) spectroscopy by using field-effect transistor device structure. The GM spectra obtained for high-mobility DA copolymer thin films exhibited second-derivative-like line shapes due to an effect of spectral broadening of ordinary exciton absorption spectra by accumulated charges. In contrast, the GM spectra obtained for relatively low-mobility DA copolymer thin films exhibited simple bleaching of exciton absorption spectra, as well as observed for non-DA-type-type polymers like poly(3-hexylthiophene-2,5-diyl) (P3HT). From a systematic comparison of the GM spectra with temperature-dependent absorption spectra for the polymers in solution, we found that the spectral broadening observed in the GM spectra can be attributed to a reduced effect on the exchange narrowing where excitonic transitions of individual polymer chains are coherently coupled within highly-ordered crystalline domains in the polymer thin films. We discuss that the gate-induced charge accumulation in the polymer films effects to suppress the exciton coherence length, which contributes to the reduced exchange narrowing. We also discuss that the whole feature of the GM spectra can be understood in terms of a decomposition into ordered and disordered polymers, and that the GM spectra can be used as fine probes for a degree of structural ordering in semiconductor channels of polymer field-effect transistors.

I. INTRODUCTION

Exciton absorption spectra of semiconducting π-conjugated polymers are strongly affected by the interchain structural order, as well as by the linear rigidity of the conjugated backbones [1,2]. The spectral linewidth becomes relatively sharp, with a value of about 0.4 eV, when the conjugated backbone is linearly extended, whereas it becomes broader than 1 eV when the backbone is folded or disordered. A particular example of a sharp exciton absorption spectrum is seen in poly(3-hexylthiophene-2,5-diyl) (P3HT), which has a crystalline lamellar structure in which the conductive layers composed of the rigid linear backbones are stacked and are separated by the alkyl side-chain layers [3,4]. Such layered-crystalline polymers have attracted considerable recent attentions, because their crystalline layer structure permits efficient carrier transport in polymer field-effect transistors (PFETs) [5].

In the absorption spectrum of P3HT, a sharp shoulder-like structure appears on the lower-energy side of the main exciton absorption when the interchain structural order is reinforced by the introduction of regioregularity [2,6–13]. It has been pointed out that the shoulder structure could be ascribed to exchange narrowing of the exciton absorption where the excitonic transitions of the individual polymer chains are coherently coupled within the crystalline domains [14–18]. The exchange narrowing effect on optical absorption and luminescence spectra is known as an outstanding and fundamental concept in some crystalline molecular materials, as is exemplified by “Davydov splitting” in polyacenes and “exchange narrowing in J-aggregates” in carotenoid, cyanine dyes, and porphyrins, where a marked spectral narrowing accompanied by a spectral shift was clearly observed [19]. In striking

contrast, the effect in polymer semiconductors has not been so evident as the crystalline molecular materials, probably because the transition moments are much smaller and disordered domains should be present within the films. Therefore, these effects have not been a crucial subject so far on polymer semiconductors.

Recently, a new series of semiconducting π-conjugated polymers has been developed in which the polymer main chain consists of an alternating sequence of electron donor and electron acceptor units. These are referred to as donor–acceptor (DA) copolymers and were reported to exhibit an excellent mobility, considerably in excess of 1 $cm^2 V^{-1} s^{-1}$, in PFETs [20–24]. These copolymers exhibit a large transition dipole moment due to donor–acceptor charge-transfer exciton absorption as well to as the high crystalline order in the films. These features lead us to expect the presence of strong interchain excitonic coupling, although this effect has not yet been disclosed.

Here, we report an effect of charge accumulation on the exciton absorption spectra for five kinds of semiconducting DA copolymers, PDPP2T-TT (abbreviated hereafter as DA1, as shown in Fig. 1) [20–22], PDVT-10 (DA2) [23–24], PNTz4T (DA3) [25], P(NDI2OD-T2) (DA4) [26], and PCPDTBT (DA5) [27], as well as for non-DA-type polymers, P3HT and PNDT3BT [28]. We used gate-modulation (GM) spectroscopy [29–32] to investigate slight variations in the exciton absorption spectra induced by the charge accumulation in the PFETs. We found that second-derivative-like line shapes due to spectral broadening of the exciton absorption spectra were clearly observed in the GM spectra of the high-mobility DA copolymers, whereas simple bleaching was observed in the GM spectra of the low-mobility

DA copolymers and the non-DA-type polymers. On the basis of the comparisons with temperature-dependent absorption spectra of the polymers in solution, we discuss that the spectral broadening observed in the GM spectra can be ascribed to a reduction of the exciton coherence length by the charge accumulation in highly-ordered domains in the polymer thin films, and that the GM spectra can be used as fine probes for a degree of structural ordering in the channels of the PFETs.

II. EXPERIMENT

The semiconducting polymers, DA3 and PNDT3BT, were synthesized by the process reported in the references [25,28], whereas the other ones were purchased from vendors; DA1, DA2, DA5 from 1-Material Inc. (Dorval, Quebec, Canada), DA4 from Polyera Corp. (Skokie, Illinois, USA), and P3HT from Merck KGaA (Darmstadt, Germany). Their molecular weights and polydispersity indices are summarized in Fig. 1. For the measurements of the GM spectra, we fabricated semitransparent thin-film PFETs on quartz glass substrates with a bottom-gate bottom-contact configuration with a channel length of 100 μm and a channel width of 1 mm (see Fig. 2a). The devices consisted of successively accumulated layers of a gold gate electrode (6 nm), a fluoropolymer layer (400 nm; CYTOP CTL-809M; Asahi Glass Co., Ltd., Tokyo) as the gate dielectric, gold source and drain electrodes (30 nm), and a thin film of semiconducting polymer (60 nm). The fluoropolymer gate dielectric was formed by a spin-coating method. The gate and source/drain electrodes were patterned by vacuum sublimation with stencil masks. Cr was used as an adhesion layer between the Au source/drain

electrode and the fluoropolymer gate dielectric as well as between the Au gate electrode and the quartz glass substrate. Al was used as an adhesion layer between the Au gate electrode and the fluoropolymer gate dielectric.

The thin films of the semiconducting polymers were formed on the highly hydrophobic fluoropolymer surface by a push-coating technique [33] in which a 0.1 wt% solution of the semiconducting polymer in 1,2,4-trichlorobenzene was dropped onto the fluoropolymer surface and was compressed by using a stamp made of viscoelastic poly(dimethylsiloxane) (PDMS). The newly prepared thin films of semiconducting polymers were annealed at 373 K for 30 min. The measured areal capacitance of the gate dielectric was 4.1×10^{-9} F cm^{-2}.

The GM measurements were conducted by using a Cassegrain-type microscope system in conjunction with a grating monochromator whose spectral resolution and focal length were 6 nm and 257.4 mm, respectively [31]. A halogen lamp was used as the light source. The incident light was focused onto the channel between the source and drain electrodes in the PFETs, and the transmitted light was detected by Si and InGaAs photodiodes. The illumination area on the PFETs was 100×100 μm^2, and the power density was about 0.2 mW cm^{-2} at 630 nm and about 1 mW cm^{-2} at 1100 nm. In the measurements, the source and drain electrodes were grounded, and a square-wave ac bias (5 V, 10 Hz) was applied to the gate electrode with a dc offset bias of −50 V for *p*-type polymers (50 V for *n*-type polymer DA4). The modulated transmittance signal (ΔT) was detected by a lock-in technique to obtain the GM signal ($\Delta\alpha d = -\Delta T/T$) where α, d, and T are the linear absorption coefficient, film thickness, and transmittance, respectively.

The absorption spectra of the polymer solutions were measured in the temperature range 303–453 K. The measurements were conducted on 1,2,4-trichlorobenzene solutions of the semiconducting polymers with the concentration of 0.002 wt%. The measurements were also conducted on nitrobenzene solutions of the semiconducting polymers with the concentration of 6×10^{-6}, 6×10^{-5}, and 2×10^{-4} wt%.

Synchrotron radiated X-ray diffraction measurements were conducted at BL-7C line of the KEK (High Energy Accelerator Research Organization) Photon Factory. The monochromatized X-ray (energy 8.9 keV, wavelength 1.388 Å) was focused on the sample film surface, and the Bragg reflections were detected by the Rigaku SmartLab diffractometer. All device fabrications and measurements, except for solution spectroscopy and X-ray diffraction, were conducted under inert N_2 gas.

III. RESULTS AND DISCUSSION

III-1. *Critical dimensions in polymers*

Firstly, we consider critical dimensions involved in the present polymer systems for a better understanding of subsequent discussions. From the molecular weight (M_w = 65 kDa), it is estimated that the single polymer chain of DA1 consists of about 59 monomer units. The length of the single polymer chain can be therefore estimated at about 108 nm with using the length of monomer unit (1.85 nm), assuming that the polymer chain is fully extended. Figure 1 shows a summary of above estimation for the seven kinds of semiconducting polymers. Optical electronic excitations of organic materials are confined exclusively to the individual

molecular units, and the dimension of relative motion of photo-generated electron–hole pairs for the excitons should be further confined to a few monomer units because of the very strong electron–hole Coulomb interactions [34].

III-2. *Gate modulation spectra*

Figure 2b shows GM spectra measured for thin-film PFETs of the seven kinds of polymers at room temperature. The magnitude relation of their mobilities was obtained as follows; DA1 > DA2 > DA3 > DA4 > P3HT ≈ PNDT3BT > DA5, as presented in Fig. 2b. As seen, a positive signal was observed at low energy region for all the polymers; < 1.45 eV for DA1, < 1.48 eV for DA2, < 1.61 eV for DA3, < 1.53 eV for DA4, < 1.57 eV for DA5, < 2.00 eV for P3HT, and < 2.23 eV for PNDT3BT. These signals can be ascribed to an increase of the exciton absorption transition from singly occupied molecular orbital (SOMO) to the lowest unoccupied molecular orbital (LUMO) for radical ionic polymers. On the other hand, a negative signal was observed at high energy region; > 1.45 eV for DA1, > 1.48 eV for DA2, > 1.61 eV for DA3, > 1.53 eV for DA4, > 1.57 eV for DA5, > 2.00 eV for P3HT, and > 2.23 eV for PNDT3BT. In the case of high-mobility DA copolymers (≥ 0.1 cm^2 V^{-1} s^{-1}), these line shapes are much sharper than those of the ordinary absorption spectra and are similar to the second derivative line shapes of the respective absorption spectra. These feature are considerably different from those for a low-mobility DA copolymer, DA5 (0.0004 cm^2 V^{-1} s^{-1}), where the spectral line shapes can be basically understood in terms of a bleaching of the exciton absorption transition from the highest occupied molecular orbital (HOMO) to the

LUMO, as well as observed for non-DA-type polymers, P3HT and PNDT3BT [30,35]. The second-derivative-like line shapes of the GM spectra indicate that the exciton absorption spectra are broadened by the charge accumulation.

Figure 3 summarizes spectral sharpness of the GM spectra where $\Delta\alpha d$ / αd and W_{GMS} / W_{abs} correspond to the peak intensity and the peak width of GM spectra both normalized by those of the ordinary absorption spectra, respectively. These parameters were estimated for the peak at 1.5 eV for DA1, 1.5 eV for DA2, 1.7 eV for DA3, 1.7 eV for DA4, 1.8 eV for DA5, 2.3 eV for P3HT, and 2.5 eV for PNDT3BT. As seen, the $\Delta\alpha d$ / αd increases, and the W_{GMS} / W_{abs} decreases, monotonically, as the mobility increases. These plots clearly indicate that the sharp second-derivative-like line shapes of the GM spectra are closely associated with the increase of the mobility. As we will show below, such a systematic variation in the GM spectra can be ascribed to the interchain structural order of the polymer films, which should be directly responsible for the carrier mobility of the PFETs.

III-3. *Temperature-dependent solution spectra*

To clarify the origin of the second-derivative-like line shape of the GM spectra in the high-mobility DA copolymers, we measured exciton absorption spectra of their polymer solutions at various temperatures. Figure 4a presents absorption spectra of DA1 in 1,2,4-trichlorobenzene solution measured at various temperatures between 303 and 453 K. The spectra showed a marked narrowing effect at about room temperature as compared with the spectra recorded at higher temperatures: A broad peak centered at 1.8 eV with the width of

0.22 eV at 453 K gradually disappeared as the temperature decreases, and a new sharp peak grew at 1.5 eV with the width of 0.11 eV at 303 K. The latter peak should be ascribed to the exciton absorption of aggregates of linear polymer backbones, as the feature is quite coincident with the absorption spectrum of the DA1 thin film. On the other hand, the former peak can be ascribed to the exciton absorption of isolated polymer chains, because the polymer is completely dissolved at high temperatures. The spectral change discussed above was reversible with respect to the heating–cooling cycle, indicating that polymer aggregates are in thermal equilibrium with isolated polymers. These observations clearly indicate that the DA1 aggregates present a strong interchain excitonic coupling, which is ascribable to the high interchain structural order and/or the large transition moment in DA1.

We also measured a concentration dependence of solution spectra at room temperature to confirm and establish the aggregate formation for DA1, the result of which is shown in Fig. 4b. Although it was difficult to prepare the solution of non-aggregated copolymers due to the low solubility of DA1, we successfully obtained it with use of nitrobenzene as solvents. As seen, the spectra exhibited a clear variation by the concentration, which was fundamentally similar to the spectral variation by the change of temperature: The sharp absorption peak due to the aggregates was observed at 1.5 eV with the increase of concentration, while broad peak due to the isolated polymers was observed at 1.8 eV only in the low-concentration solution. The results clearly indicate that the aggregates are formed with an increase of the concentration. Nonetheless, we used the temperature dependence of polymer solution spectra in 1,2,4-trichlorobenzene for the subsequent analyses, because it exhibited clear spectra of the

aggregates with minimized spectral component due to isolated polymers.

III-4. *Exciton coherence length analyses for highly-ordered DA1 copolymer*

A comparison of the GM spectra with the narrowing effects in the polymer solution spectra indicates that the second-derivative-like GM spectra might be due to broadening as a result of charge accumulation with gate voltages. A possible origin of this phenomenon is that the coherent interchain excitonic coupling is violated by charge accumulation in the crystalline polymer aggregates.

Such a spectral narrowing of the exciton absorption caused by coherent excitonic coupling has been previously discussed for some small-molecule organic dye crystalline materials, such as merocyanine J-aggregates [19]; if the dye molecules form a well-ordered crystalline system, electronic excitations of individual molecules are coherently coupled, leading to the formation of an exciton band, as shown in Fig. 5a [14–17]. The excited states at the wavenumber k = 0 correspond to the excited state in which the electronic transitions of individual molecules are coupled in parallel, leading to a shift in the lowest optically allowed exciton transition to a lower energy than that of the isolated molecule (Fig. 5b). The outstanding feature is the spectral narrowing effect by J-aggregate formation, in which the narrowed linewidth can be expressed by the following equation [36]:

$$w = \frac{w_0}{\sqrt{L_{\mathrm{coh}}}} \tag{1}$$

where L_{coh} is the coherence length (unit: molecules) of excitonic coupling. w is the spectral

linewidth of a molecular aggregate, and w_0 is the spectral linewidth of an isolated molecule. The relevant physics behind Eq. 1 was firstly introduced as "motional narrowing" in the field of nuclear magnetic resonance where the fluctuating local magnetic fields created by randomly oriented nuclear spins are averaged when the motion of the nuclei is thermally activated [37]. Inspired by this, the similar concept was proposed as "exchange narrowing" in the field of optical spectroscopy where the delocalized exciton state of the aggregate averages over the local inhomogeneities in the transition energies of the individual molecules [36,38]. The simple explanation of Eq. 1 can be given by considering the probability distribution of each of the transition energies: Averaging transition energies of L_{coh} molecules gives square root dependence on L_{coh}.

The exciton coherence length can be estimated by means of Eq. 1, by comparison of the spectral linewidths with and without the exchange-narrowing effect. Here we estimate the exciton coherence length for the DA1 solution from the temperature-dependent spectra (Fig. 4a). The exciton coherence length was estimated by the following procedure. First, the spectrum at 453 K was assigned to the absorption of the isolated polymers, because the absorption of polymer aggregates completely disappears above this temperature. The spectrum at 453 K was then used to fit the solution spectra at temperatures other than 453 K, and the residual spectral components were extracted and assumed to correspond to absorption by polymer aggregates (see inset to Fig. 6a). Figure 6a shows the fraction of polymer aggregates, as estimated by spectral fitting. This fraction increased with decreasing temperature, and the variation was almost saturated below 400 K, indicating that aggregates

become dominant below 400 K. The inset to Fig. 6b shows the spectral components for the polymer aggregates. The vibrational progressions were well fitted by three Gaussians with an interval of 0.14 eV. Figure 6b shows the variation in the peak position and linewidth of the aggregates. The spectral components for the polymer aggregates clearly show a peak shift from 1.58 eV to 1.50 eV and a linewidth reduction from 0.15 eV to 0.11 eV in the temperature range between 433 and 303 K. From the obtained peak linewidth, we estimated the exciton coherence length, L_{coh}, at the respective temperatures by using Eq. 1 (Fig. 6c). The exciton coherence length increases at low temperatures and is extended over four molecules at 303 K. This trend can be ascribed to dimensional growth of polymer aggregates at low temperatures. The exciton coherence length of four molecules corresponds to a length of 1.5 nm if the co-facial separation (0.38 nm) between the nearest-neighbor polymer chains is used. The exciton coherence length of the thin film was also estimated by comparison of the linewidth of absorption spectra between the thin film and the isolated polymers in solution. As seen in Fig. 6d, the linewidth of the thin film (0.13 eV) is clearly smaller than that of the isolated polymers in solution (0.22 eV), which gives the exciton coherence length of three molecules (1.1 nm).

In addition to the spectral narrowing, the extended exciton coherence can also be confirmed by the relative intensity distribution among the vibrational subbands. It is known that a change in exciton coherence length could cause a variation of relative intensity distribution among the vibrational subbands, e.g., enhancement of the 0-0 vibronic peak intensity for the case of J-aggregate-type excitonic coupling [2,8–11,18]. We checked the vibronic peak

intensity of the polymer aggregates formed in the solution, and found that the 0-0 vibronic peak intensity was strongly enhanced. As seen in the inset of Fig. 4b, the 0-0 vibronic peak intensity is about 2 times larger than the 0-1 vibronic peak intensity, indicating the strong J-aggregate-type excitonic coupling. This is fairly consistent with the extended exciton coherence length estimated from the spectral narrowing.

It should be necessary to consider here that the spectral narrowing could be affected by other effects than the exchange narrowing. Particularly, we have to consider the electron-phonon coupling effect, because absorption spectra are the convolution between vibrational progression due to the electron-phonon coupling and inhomogeneous broadening of optical transition. It is known that the electron-phonon coupling causes the variation of relative intensity distribution among the vibrational subbands by the change of temperature. However, the effect does not cause the linewidth variation of each subband in general [39]. It is therefore clear that the linewidth narrowing of each subband observed in this work (Fig. 6b) cannot be ascribed to the electron-phonon coupling. On the other hand, it has been reported for the π-conjugated polymers that the temperature dependent inhomogeneous broadening could be caused by thermally induced torsional displacement of polymer main chains which strongly affects effective π-conjugation length along the polymer main chain [40,41]. This effect is well observed in non-aggregated polymer solutions where the polymer chain is free to be transformed. However, the effect is not observed in aggregated polymer solution (or in solid state polymer) where torsional displacement should be frozen. For example, poly[2-methoxy-5-(2-ethylhexyloxy)-1,4-phenylenevinylene] (MEH-PPV) demonstrates no

spectral narrowing in the thin film, whereas it demonstrates spectral narrowing of 20 meV in the temperature range from 300 K to 200 K in the non-aggregated solution [40]. Thus, neither the torsional displacement effect nor the electron-phonon coupling effect gives the reasonable explanation of the spectral narrowing observed for polymer aggregates (Fig. 6b). From the above considerations, the exchange narrowing effect should be the most probable origin for the spectral narrowing observed in the aggregated solution of DA1.

III-5. *Coexistence of ordered and disordered polymers; further spectral analyses*

The spectral narrowing observed in the solution spectra provides convincing evidence that the second-derivative-like spectral line shape of the GM spectra probably originates from a reduction in exciton coherence length as a result of charge accumulation, which contributes to a reduction in the exchange-narrowing effect. To understand the charge-induced reduction of the exciton coherence length, we compared the GM spectrum with the solution spectra.

Figure 7a shows the change in the absorption spectra with changing temperature for a 1,2,4-trichlorobenzene solution of DA1 as obtained by subtracting the lower-temperature spectrum from the higher-temperature spectrum: $\Delta\varepsilon_{HT}$ corresponds to the difference spectrum at high temperatures between 433 K and 423 K, and $\Delta\varepsilon_{LT}$ corresponds to that at low temperatures between 303 K and 313 K. These difference spectra can be regarded as the spectral changes induced by the reduction in exciton coherence length: $L_{coh} = 2.6 \rightarrow 2.3$ for $\Delta\varepsilon_{HT}$ and $L_{coh} = 4.0 \rightarrow 3.9$ for $\Delta\varepsilon_{LT}$ (see Fig. 6c). As can be seen, $\Delta\varepsilon_{LT}$ shows a second-derivative-like spectral shape that closely resembles the GM spectrum. This clearly

indicates that the exciton coherence length is reduced by charge accumulation. The coherence reduction by charge accumulation can be considered as follows. The charge accumulation (with the density of 1.3×10^{11} cm^{-2} for the measurements of GM spectra) ionizes a small minority of polymers in the PFET. The ionized polymers do not show the exciton coupling with the neutral polymers because their transition energies should be different from those of the neutral polymers [35]. As a result, if we assume that a charge carrier is injected into a thin film consisting of crystalline domains with the exciton coherence length of L_{coh}, the exciton coherence length of the charge-injected domain should decrease from L_{coh} to ($L_{coh} - 1$), as shown in Fig. 5c, whereas those of the other domains remain unchanged. Because the coherence reduction increases the spectral linewidth by a factor of $\sqrt{L_{coh}/(L_{coh}-1)}$, in accordance with Eq. 1, the spectral change should have a second-derivative-like spectral line shape. On the other hand, if a charge carrier is injected into the disordered thin film with $L_{coh} = 1$, the exciton coherence length remains unchanged before and after charge injection. In this case, the absorption of the neutral polymer disappears as a result of ionization, and the spectral change should therefore correspond to simple bleaching of the absorption. The second-derivative-like spectral shape in the GM spectrum for DA1 PFETs can be well understood by the mechanism discussed above.

Note, however, that the GM spectrum of DA1 coincides quite well with the summed spectra of $\Delta\varepsilon_{HT}$ and $\Delta\varepsilon_{LT}$ in a ratio of about 2:5 (Fig. 7b). This indicates that the DA1 film is composed of two different domains whose exciton coherence length are $L_{coh} = 4.0$ and $L_{coh} = 2.6$, respectively (Fig. 7c). These values are consistent with the exciton coherence length (L_{coh}

= 3.0) estimated from the linewidth analysis of the regular absorption spectra (Fig. 6d). As a plausible structural model, the thin film of DA1 can be considered as consisting of well-ordered domains that are partly surrounded by disordered domains, as reported for other polymer semiconductors [42]. The disordered domains might act as local charge-trapping sites and thereby limit interdomain charge transport.

The relation between the structural order and the exciton coherence length was examined by using the synchrotron radiated X-ray diffraction measurements. Figure 8a shows the out-of-plane and in-plane X-ray diffractions measured for the thin film of DA1. As seen, the diffraction peaks were observed both in the out-of-plane and in-plane setups, indicating that the ordered structure responsible for the exciton coherence should be formed in the film. The peaks in the out-of-plane setup (q = 2.7 and 5.4 nm^{-1}) correspond to the first and higher order diffractions from the 2.30 nm d-spacing, while the peak in the in-plane setup (q = 16.5 nm^{-1}) corresponds to the diffraction from the 0.38 nm d-spacing. These d-spacings indicate that the film of DA1 demonstrates a lamellar structure in which the conductive layers composed of the parallel π-stacked polymers with the co-facial separation of 0.38 nm are separated by the alkyl side-chain layers with the interlayer distance of 2.30 nm (Fig. 8b). By using the Scherrer's equation [43], the size of crystalline grains are roughly estimated at 11 nm from the peak width of the out-of-plane diffraction (q = 2.7 nm^{-1}). Such structural order is responsible for the extended exciton coherence length obtained from the GM spectrum (1.52 nm, L_{coh} = 4.0).

IV. CONCLUSIONS

In summary, we have systematically investigated the effect of charge accumulation on the exchange narrowing of the exciton absorption spectra of various DA copolymers. The GM spectra, measured for thin-film transistors with the high-mobility DA copolymers as the semiconductor channel, were well fitted by the second-derivative-like line shape of the absorption spectra in sharp contrast to those of the low-mobility polymers. This result indicates that the absorption spectrum is broadened by a reduction in exchange narrowing caused by charge accumulation. From a comparison with the temperature-dependent absorption spectra of the polymer solution, we demonstrated that the reduced exchange narrowing originates from coherence reduction of interchain excitonic coupling due to the accumulated charges. We also demonstrated that the exciton coherence length extended to four molecules in the solid-state DA1. This finding should be important in understanding the spectroscopic signature of excitonic absorption for molecular solids, particularly for well-ordered systems with extended exciton coherence length which is a key factor in developing high-performance PFETs.

ACKNOWLEDGEMENTS

We are grateful to Prof. Kazuo Takimiya (RIKEN Center for Emergent Matter Science) for providing PNTz4T (DA3) and PNDT3BT. X-ray diffraction study was performed under the approval of the Photon Factory Program Advisory Committee (Proposal No. 2014S2-001). This work was supported by Japan Society for The Promotion of Science (JSPS) KAKENHI (Grant Number: 16H05976) and by the Japan Science and Technology Agency (JST) through

the Strategic Promotion of Innovative Research and Development Program (S-Innovation).

REFERENCES

[1] T. Tokihiro and E. Hanamura, Phys. Rev. Lett. **71**, 1423 (1993).

[2] J.-F. Chang, J. Clark, N. Zhao, H. Sirringhaus, D. W. Breiby, J. W. Andreasen, M. M. Nielsen, M. Giles, M. Heeney, and I. McCulloch, Phys. Rev. B **74**, 115318 (2006).

[3] R. D. McCullough, Adv. Mater. (Weinheim, Ger.) **10**, 93 (1998).

[4] R. D. McCullough, S. Tristram-Nagle, S. P. Williams, R. D. Lowe, and M. Jayaraman, J. Am. Chem. Soc. **115**, 4910 (1993).

[5] H. Sirringhaus, P. J. Brown, R. H. Friend, M. M. Nielsen, K. Bechgaard, B. M. W. Langeveld-Voss, A. J. H. Spiering, R. A. J. Janssen, E. W. Meijer, P. Herwig, and D. M. de Leeuw, Nature **401**, 685 (1999).

[6] P. J. Brown, D. S. Thomas, A. Köhler, J. S. Wilson, J.-S. Kim, C. M. Ramsdale, H. Sirringhaus, and R. H. Friend, Phys. Rev. B **67**, 064203 (2003).

[7] F. C. Spano, J. Chem. Phys. **122**, 234701 (2005).

[8] J. Clark, C. Silva, R. H. Friend, and F. C. Spano, Phys. Rev. Lett. **98**, 206406 (2007).

[9] J. Clark, J.-F. Chang, F. C. Spano, R. H. Friend, and C. Silva, Appl. Phys. Lett. **94**, 163306 (2009).

[10] F. C. Spano, J. Clark, C. Silva, and R. H. Friend, J. Chem. Phys. **130**, 074904 (2009).

[11] F. Paquin, H. Yamagata, N. J. Hestand, M. Sakowicz, N. Bérubé, M. Côté, L. X. Reynolds, S. A. Haque, N. Stingelin, F. C. Spano, and C. Silva, Phys. Rev. B **88**, 155202

(2013).

[12] F. Panzer, H. Bässler, R. Lohwasser, M. Thelakkat, and A. Köhler, J. Phys. Chem. Lett. **5**, 2742 (2014).

[13] F. Panzer, M. Sommer, H. Bässler, M. Thelakkat, and A. Köhler, Macromolecules **48**, 1543 (2015).

[14] A. S. Davydov, *Theory of Molecular Excitons* (McGraw-Hill, New York, 1962).

[15] M. Kasha, NATO Adv. Study Inst. Ser., Ser. B **12**, 337 (1976).

[16] R. M. Hochstrasser and M. Kasha, Photochem. Photobiol. **3**, 317 (1964).

[17] E. G. McRae and M. Kasha, in *Physical Processes in Radiation Biology*, proceedings of the international symposium, Michigan State University, (Academic, New York, 1964), p. 23; DOI: 10.1016/B978-1-4831-9824-8.50007-4

[18] F. C. Spano, Acc. Chem. Res. **43**, 429 (2010).

[19] *J-Aggregates*, edited by T. Kobayashi (World Scientific, Singapore, 1996).

[20] D. Venkateshvaran, M. Nikolka, A. Sadhanala, V. Lemaur, M. Zelazny, M. Kepa, M. Hurhangee, A. J. Kronemeijer, V. Pecunia, I. Nasrallah, I. Romanov, K. Broch, I. McCulloch, D. Emin, Y. Olivier, J. Cornil, D. Beljonne, and H. Sirringhaus, Nature **515**, 384 (2014).

[21] J. Li, Y. Zhao, H. S. Tan, Y. Guo, C.-A. Di, G. Yu, Y. Liu, M. Lin, S. H. Lim, Y. Zhou, H. Su, and B. S. Ong, Sci. Rep. **2**, 754 (2012).

[22] W. Li, K. H. Hendriks, W. S. C. Roelofs, Y. Kim, M. M. Wienk, and R. A. J. Janssen, Adv. Mater. (Weinheim, Ger.) **25**, 3182 (2013).

[23] H. Chen, Y. Guo, G. Yu, Y. Zhao, J. Zhang, D. Gao, H. Liu, and Y. Liu, Adv. Mater. (Weinheim, Ger.) **24**, 4618 (2012).

[24] I. Kang, H.-J. Yun, D. S. Chung, S.-K. Kwon, and Y.-H. Kim, J. Am. Chem. Soc. **135**, 14896 (2013).

[25] I. Osaka, M. Shimawaki, H. Mori, I. Doi, E. Miyazaki, T. Koganezawa, and K. Takimiya, J. Am. Chem. Soc. **134**, 3498 (2012).

[26] H. Yan, Z. Chen, Y. Zheng, C. Newman, J. R. Quinn, F. Dötz, M. Kastler, and A. Facchetti, Nature **457**, 679 (2009).

[27] D. Mühlbacher, M. Scharber, M. Morana, Z. Zhu, D. Waller, R. Gaudiana, and C. Brabec, Adv. Mater. **18**, 2884 (2006).

[28] I. Osaka, S. Shinamura, T. Abe, and K. Takimiya, J. Mater. Chem. C **1**, 1297 (2013).

[29] Y. Y. Deng and H. Sirringhaus, Phys. Rev. B **72**, 045207 (2005).

[30] D. Beljonne, J. Cornil, H. Sirringhaus, P. J. Brown, M. Shkunov, R. H. Friend, and J.-L. Brédas, Adv. Funct. Mater. **11**, 229 (2001).

[31] S. Haas, H. Matsui, and T. Hasegawa, Phys. Rev. B **82**, 161301(R) (2010).

[32] J. Tsutsumi, S. Matsuoka, T. Yamada, and T. Hasegawa, Org. Electron. **25**, 289 (2015).

[33] M. Ikawa, T. Yamada, H. Matsui, H. Minemawari, J. Tsutsumi, Y. Horii, M. Chikamatsu, R. Azumi, R. Kumai, and T. Hasegawa, Nat. Commun. **3**, 1176 (2012).

[34] T. Hasegawa, Y. Iwasa, H. Sunamura, T. Koda, Y. Tokura, H. Tachibana, M. Matsumoto, and S. abe, Phys. Rev. Lett. **69**, 668 (1992).

[35] G. Horowitz, A. Yassar, and H. J. von Bardeleben, Synth. Met. **62**, 245 (1994).

[36] E. W. Knapp, Chem. Phys. **85**, 73 (1984).

[37] R. Celotta and J. Levine, *Methods of Experimental Physics vol. 21* (Academic Press, London, 1983).

[38] J. Knoester, J. Chem. Phys. **99**, 8466 (1993).

[39] H. Suzuki, *Electronic Absorption Spectra and Geometry of Organic Molecules* (Academic Press, New York, 1967).

[40] S. T. Hoffmann, H. Bässler, and A. Köhler, J. Phys. Chem. B **114**, 17037 (2010).

[41] W. Barford and D. Trembath, Phys. Rev. B **80**, 165418 (2009).

[42] B. Watts, T. Schuettfort, and C. R. McNeill, Adv. Funct. Mater. **21**, 1122 (2011).

[43] P. Scherrer, Göttinger Nachrichten. **2**, 98 (1918).

FIGURE CAPTIONS

Figure 1

Molecular structures, molecular weights (M_w), poly dispersity indices (PDI), lengths of monomer unit, and lengths of polymer chain for seven kinds of semiconducting polymers.

Figure 2

(a) Schematic device structure of a thin-film transistor. (b) GM spectra measured for thin-film transistors with seven kinds of semiconducting polymers as the semiconductor channels (black line). The red and blue lines are the absorption spectra measured for the thin films and their second derivatives, respectively.

Figure 3

Peak Intensity ($\Delta\alpha d$ / αd) and peak width (W_{GMS} / W_{abs}) of the GM spectra normalized by those of the ordinary absorption spectra. Both parameters are plotted as a function of carrier mobility.

Figure 4

(a) Temperature dependence of the absorption spectra measured for a 1,2,4-trichlorobenzene solution of DA1, in which the molar absorption coefficient (ε) is plotted as a function of the photon energy. The absorption spectrum measured for the thin film is shown for comparison (broken line). (b) Concentration dependence of the absorption spectra measured for

nitrobenzene solutions of DA1 at room temperature.

Figure 5

(a) Schematic representation of the electronic structure of an isolated polymer and a polymer aggregate, in which the ground and excited states are abbreviated as GS and ES, respectively. (b) Schematic representation of absorption spectra for an isolated polymer and a polymer aggregate. (c) Mechanisms of charge-induced changes in the absorption spectra for ordered and disordered polymer aggregates.

Figure 6

(a) Fraction of polymer aggregates in the DA1 solution, as estimated from the spectral fitting. The inset shows spectral components of the polymer aggregates and isolated polymers obtained by fitting of the solution spectrum measured at 413 K. (b) Peak position and width for spectral component of polymer aggregates, as determined by Gaussian fitting. The inset shows the spectral component of polymer aggregates at 303 K whose vibrational progressions are fitted by three Gaussians. (c) Exciton coherence length L_{coh} estimated from the peak width of the polymer aggregates. (d) Absorption spectra measured for a 1,2,4-trichlorobenzene solution of DA1 at 453 K and a thin film of DA1 at room temperature. The red lines are vibrational progressions fitted by Gaussians.

Figure 7

(a) Difference spectra for two different temperatures for the DA1 solution; $\Delta\varepsilon_{HT}$ between 423 K and 433 K and $\Delta\varepsilon_{LT}$ between 303 K and 313 K. (b) A summed spectrum of $\Delta\varepsilon_{HT}$ and $\Delta\varepsilon_{LT}$ with a ratio of 2:5 (red line), and a GM spectrum of a thin film of DA1 (black line). (c) Schematic representation of a DA1 thin film consisting of high- and low-coherence domains.

Figure 8

(a) Out-of-plane and in-plane X-ray diffractions measured for the thin film of DA1. Background halo pattern due to a quartz glass substrate is subtracted for the shown data. (b) Schematic for lamellar structure of DA1.

FIGURES

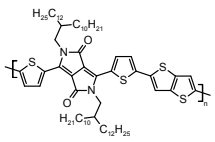

DA1

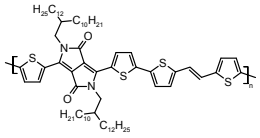

DA2

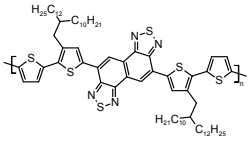

DA3

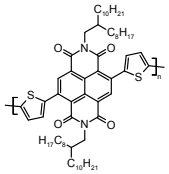

DA4

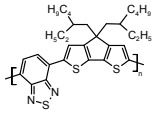

DA5

P3HT

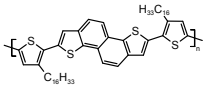

PNDT3BT

	DA1	DA2	DA3	DA4	DA5	P3HT	PNDT3BT
M_w (kDa)	65	50	127	178	41	71	46
PDI	2.4	2.3	2.4	3.7	2.3	1.7	1.6
Length of monomer unit (nm)	1.85	2.28	2.31	1.51	1.28	0.49	1.86
Length of polymer chain (nm)	108	98	236	271	96	210	100

Figure 1. Tsutsumi et al.

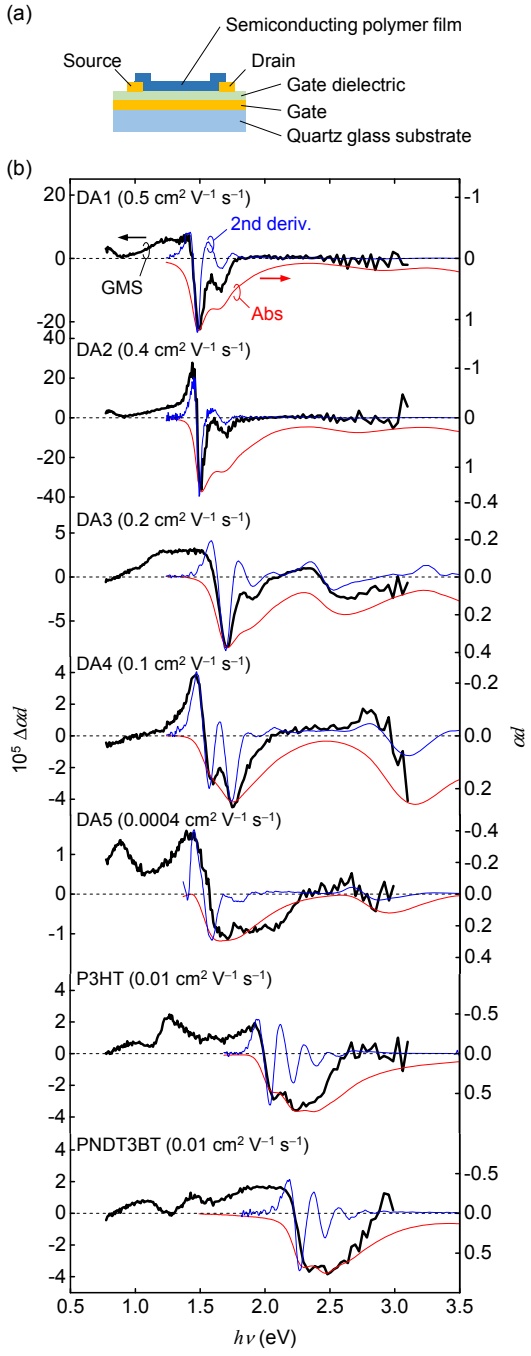

Figure 2. Tsutsumi et al

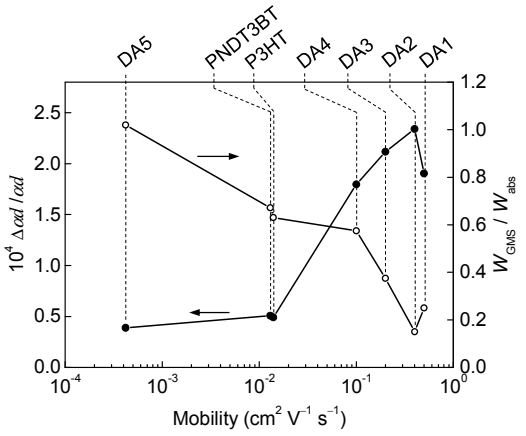

Figure 3. Tsutsumi et al

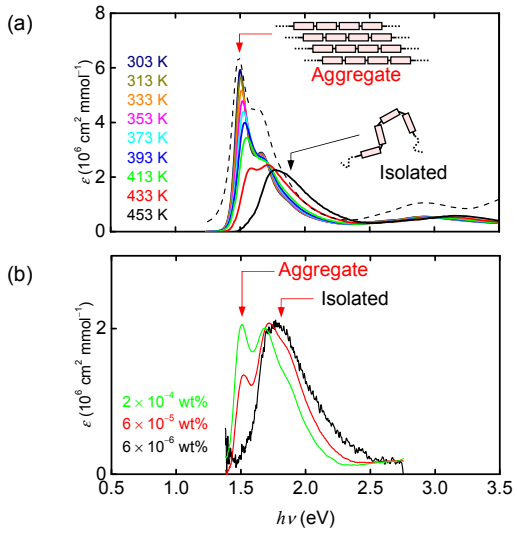

Figure 4. Tsutsumi et al

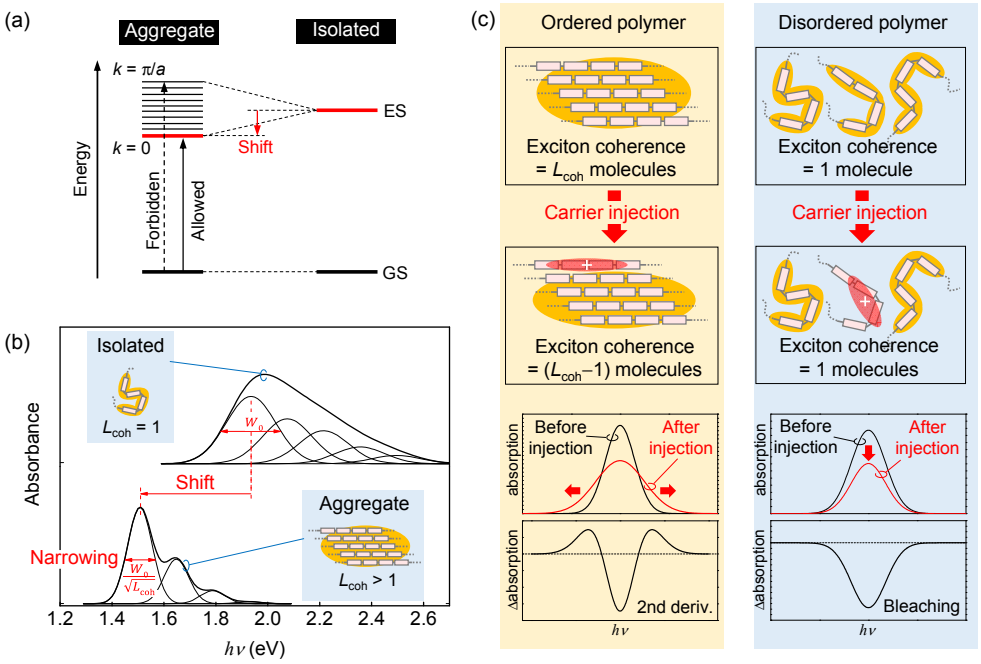

Figure 5. Tsutsumi et al.

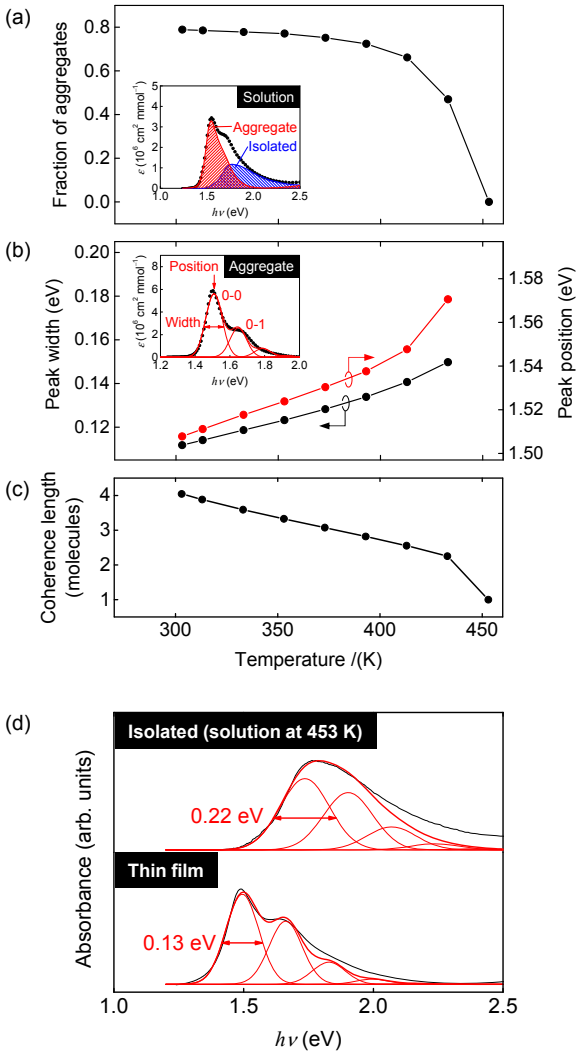

Figure 6. Tsutsumi et al.

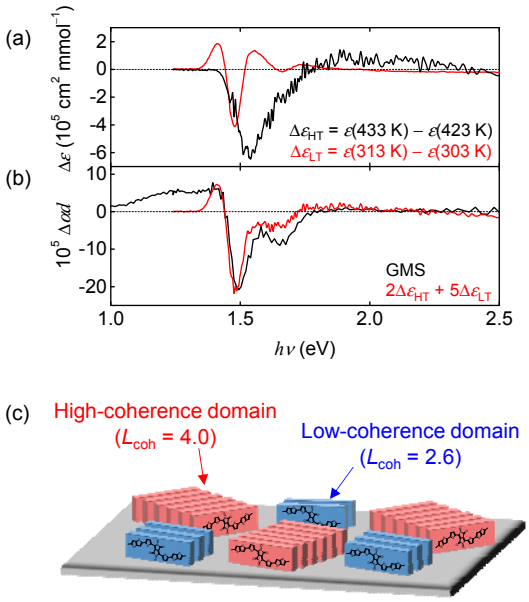

Figure 7. Tsutsumi et al.

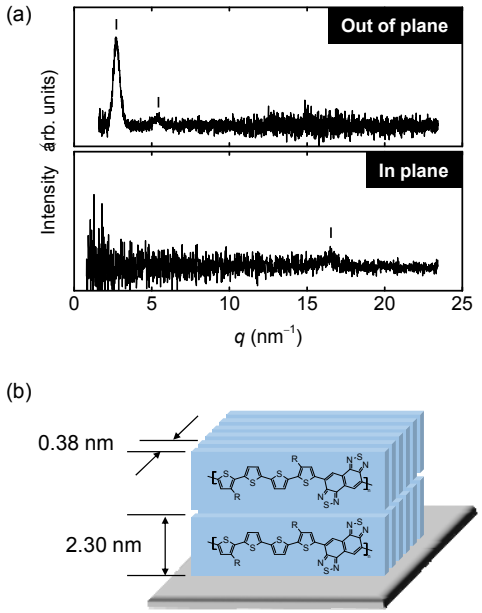

Figure 8. Tsutsumi et al.